Institut für Kernphysik der Universität Frankfurt/Main

Zero and First Sound in NaF and RbI

By

A. Loidl, H. Jex, J. Daubert[1]), and M. Müllner

Zero and first sound as well as the transition region are investigated theoretically in RbI and NaF. The temperature dependence of the first sound, zero sound, and isothermal elastic constants is calculated on the basis of a breathing shell model for the harmonic lattice dynamics and anharmonic parameters from microscopic Grüneisen constants. The theoretical results are compared with ultrasonic data and inelastic neutron scattering results. Own recent neutron experiments in RbI are concerned with the zero sound region at room temperature while the NaF experiments cover also parts of the transition region between first and zero sound at various temperatures between 295 and 700 K. It is shown that the dispersion of sound is satisfactorily described by use of an averaged thermal phonon lifetime. In NaF for each temperature first sound elastic constants and averaged phonon lifetimes are deduced from an analysis of the experimental data.

Der nullte und erste Schall in NaF and RbJ sowie der Übergangsbereich werden theoretisch untersucht und mit neuesten Experimenten verglichen. Die Temperaturabhängigkeit der isothermen elastischen Konstanten und der elastischen Konstanten aus dem Bereich des nullten und ersten Schalls wird berechnet, wobei die harmonische Gitterdynamik mit einem Breathing-Shell-Modell beschrieben wird und die anharmonischen Parameter aus einer Analyse der mikroskopischen Grüneisen-Konstanten bestimmt werden. Die Ergebnisse werden mit Ultraschalldaten und inelastischer Neutronenstreuung verglichen. Die Rechnungen beziehen sich auf eigene Neutronenexperimente aus dem Bereich des nullten Schalls in RbJ bei Zimmertemperatur und zusätzlich aus dem Übergangsbereich zum ersten Schall in NaF bei verschiedenen Temperaturen zwischen 295 und 700 K. Es wird gezeigt, daß eine mittlere Lebensdauer für die thermisch angeregten Phononen im Kristall den experimentellen Effekt gut beschreibt. Für NaF werden für jede Temperatur sowohl elastische Konstanten aus dem Bereich des ersten Schalls als auch die mittleren Lebensdauern der thermischen Phononen des Kristalls aus den experimentellen Daten ermittelt.

1. Introduction

In anharmonic crystals the mode of propagation of sound waves changes at sufficiently low frequencies, depending on the relation between the applied frequency Ω and the averaged inverse lifetime Γ of the thermal phonons in the crystal [1, 2]. In the region $\Omega \ll \Gamma$ the period of the sound wave is much longer than the lifetimes of the thermal phonons. In this case it is necessary to take account of the lifetimes of the modes and since there are many phonon collisions within each period of the sound wave a local thermal equilibrium is established in the rarefied and compressed regions of the wave. The resulting different temperatures do not have time enough to equalize. Therefore, low-frequency waves travel at adiabatic or first sound velocities. In the high frequency limit $\Omega \gg \Gamma$ the probe interacts with harmonic phonons and the local temperature of the crystal is unaffected by the presence of the phonon. High-frequency waves

[1]) Now at Physik-Department, TU München, BRD.

travel at zero sound velocities, which are expected to be slightly higher than first sound velocities [1, 3].

In terms of elastic constants the theory predicts also a different temperature dependence of zero and first sound elastic constants due to the different coupling. The difference, however, tends to zero at zero K and increases linearly with rising temperature. The transition region between the two regimes must be observed at frequencies around $\Omega \approx \Gamma$ which is typically of the order of 10^{11} s^{-1} for alkali halide crystals at room temperature. As a consequence, phonon frequencies determined from inelastic neutron scattering are usually measured in the zero sound region, while ultrasonic experiments investigate the first sound region. Actually in some favourable cases ultrasonic measurements covered also the transition region [2, 4]. Principally this region can also be studied by Brillouin scattering of light [5].

The difference in the temperature gradients of zero and first sound was observed by Svensson and Buyers [6] in KBr who compared ultrasonic and neutron data at 95 and 463 K. The experimental result was in rough agreement with Cowley's theory [1], that predicted a 10% difference between some zero and first sound elastic constants at room temperature. Blinick and Maris [2] measured sound velocities in quartz with ultrasonic techniques at different frequencies; the velocity change was of the order of 10^{-3}% at 40 K. Attempts have also been made to observe zero and first sound elastic constants in solid krypton utilizing Brillouin scattering and inelastic neutron scattering near the triple point [7]. The difference was as much as 12%.

We have concentrated our investigations on NaCl-type crystals. In these crystals often differences of the order of 10% between neutron and ultrasonic elastic constants can be found in the literature [8, 9]. We have investigated RbI and NaF in more detail theoretically in order to compare our results with recent neutron experiments by Loidl et al. [10] covering for the first time the transition region at different temperatures in NaF. Therefore, existing theories can be proved. Some additional and also necessary information was available when we started the numerical work. Thus, the phonon dispersion was determined by Raunio and Rolandson [11] for RbI and by Buyers [9] for NaF. Especially in RbI the deviation between ultrasonic elastic constants and neutron data was obvious; it reached 10% for C_{11} and 30% for C_{12} and C_{44}. The microscopic Grüneisen parameters, which determine the coupling constants of the long-wavelength phonon mass operators, have been investigated in recent theoretical work by Jex [12] and Kress [13] and experimentally by Blaschko et al. [14]. NaF was the first alkali halide crystal where second sound was observed [15].

2. Theory

The temperature dependence of the elastic constants is governed by two effects, which may be characterized as a static effect caused by thermal expansion of the crystal and a dynamic effect depending on phonon–phonon collisions. This second effect is different in the first and zero sound region. In the first sound regime dynamical renormalization treated on the basis of perturbation theory with three- and four-phonon processes is determined by colliding modes with non-negligible lifetimes. An additional correction arises from the adiabatic propagation of the first sound waves. On the other hand, it is sufficient

to treat the zero sound regime with harmonic phonons in the collision, that means the lifetime of the thermal phonons in the crystal may be neglected.

In the following we summarize briefly these ideas and discuss the different contributions to the elastic constants. We treat crystals with cubic symmetry and first define isothermal elastic constants

$$C^{\mathrm{is}}_{\alpha\beta\gamma\delta}(T) = C^{\mathrm{harm}}_{\alpha\beta\gamma\,\delta}(0) + \sum_{i=1}^{5} C^{(i)}_{\alpha\beta\gamma\delta}(T)\,. \tag{1}$$

$C^{\mathrm{harm}}_{\alpha\beta\gamma\delta}(0)$ defines the harmonic contribution to the elastic constants at 0 K. $C^{(1)}_{\alpha\beta\gamma\delta}(T)$ results from the thermal expansion and was given by E. R. Cowley and R. A. Cowley [16]

$$\left.\begin{aligned} C^{(1)}_{11}(T) &= \eta^T(2C_{11} + 2C_{12} + 6C_{111} + 4C_{112})\,, \\ C^{(1)}_{12}(T) &= \eta^T(-C_{11} - C_{12} + C_{123} + 4C_{112})\,, \\ C^{(1)}_{44}(T) &= \eta^T(C_{11} + 2C_{12} + C_{44} + \tfrac{1}{2}C_{144} + C_{166}) \end{aligned}\right\} \tag{2}$$

with the thermal strain

$$\eta^T = \frac{\hbar}{2(C_{11} + 2C_{12})}\,\frac{1}{N v_{\mathrm{a}}} \sum_{\boldsymbol{q}j} \omega\left(\begin{matrix}\boldsymbol{q}\\ j\end{matrix}\right)\gamma\left(\begin{matrix}\boldsymbol{q}\\ j\end{matrix}\right)\left(2n\left(\begin{matrix}\boldsymbol{q}\\ j\end{matrix}\right)+1\right). \tag{3}$$

The phonon Grüneisen parameter $\gamma\left(\begin{matrix}\boldsymbol{q}\\ j\end{matrix}\right)$ is introduced as the trace of the matrix defined by the microscopic Grüneisen parameters

$$\begin{aligned}\gamma^{jj'}_{\alpha\beta}(\boldsymbol{q}) = {} & \frac{3}{6\omega\left(\begin{matrix}\boldsymbol{q}\\ j\end{matrix}\right)\omega\left(\begin{matrix}\boldsymbol{q}\\ j'\end{matrix}\right)}\,\frac{1}{2}\sum_{kk'}\sum_{\gamma\delta}\left\{\varphi^{kk'}_{\gamma\delta\alpha,\,\beta}(0)\left[m_k^{-1}e_\gamma\left(k\,\middle|\,\begin{matrix}\boldsymbol{q}\\ j\end{matrix}\right)e^*_\delta\left(k\,\middle|\,\begin{matrix}\boldsymbol{q}\\ j'\end{matrix}\right)+\right.\right. \\ & + m_{k'}^{-1}e_\gamma\left(k'\,\middle|\,\begin{matrix}\boldsymbol{q}\\ j\end{matrix}\right)e^*_\delta\left(k'\,\middle|\,\begin{matrix}\boldsymbol{q}\\ j'\end{matrix}\right)\Big]- \\ & \left.\left. - \varphi^{kk'}_{\gamma\delta\alpha,\,\beta}(\boldsymbol{q})\,(m_k m_{k'})^{-1/2}\left[e_\gamma\left(k\,\middle|\,\begin{matrix}\boldsymbol{q}\\ j\end{matrix}\right)e^*_\delta\left(k'\,\middle|\,\begin{matrix}\boldsymbol{q}\\ j'\end{matrix}\right)+ e_\gamma\left(k'\,\middle|\,\begin{matrix}\boldsymbol{q}\\ j\end{matrix}\right)e^*_\delta\left(k\,\middle|\,\begin{matrix}\boldsymbol{q}\\ j'\end{matrix}\right)\right]\right\}\end{aligned} \tag{4}$$

with the Fourier transformed third derivative of the crystal potential

$$\varphi^{kk'}_{\alpha\beta\gamma,\,\delta}(\boldsymbol{q}) = \sum_{l-l'}\varphi_{\alpha\beta\gamma}\left(\begin{matrix}l\,l'\\ k\,k'\end{matrix}\right)x_\delta\left(\begin{matrix}l\,l'\\ k\,k'\end{matrix}\right)\mathrm{e}^{\,i\boldsymbol{q}\boldsymbol{x}\left(\begin{matrix}l\,l'\\ k\,k'\end{matrix}\right)}. \tag{5}$$

These elements have been explicitly derived in a calculation of the Grüneisen parameters of rubidium halides by Jex [12]. In this case the index ($\gamma = \delta$) is needed. The remaining contributions to the isothermal elastic constants are resulting from phonon–phonon interactions [16]

$$C^{(2)}_{\alpha\beta\gamma\delta}(T) = \frac{1}{N v_{\mathrm{a}}}\sum_{\boldsymbol{q}j} V_{\alpha\beta\gamma\delta}\left(-,\,-,\,\begin{matrix}\boldsymbol{q} & -\boldsymbol{q}\\ j & j\end{matrix}\right)\left[2n\left(\begin{matrix}\boldsymbol{q}\\ j\end{matrix}\right)+1\right] \tag{6}$$

with a fourth-order anharmonic coefficient

$$V_{\gamma\varepsilon\delta\varrho}\left(-,-,\begin{matrix}\boldsymbol{q} & -\boldsymbol{q}\\ j & j\end{matrix}\right)=$$

$$=\frac{\hbar}{4\omega\left(\begin{matrix}\boldsymbol{q}\\ j\end{matrix}\right)}\frac{1}{2}\sum_{\substack{\alpha\beta\\ kk'}}\left\{\varphi^{kk'}_{\alpha\beta\gamma\varepsilon\delta\varrho}(0)\left[m_k^{-1}e_\alpha\left(k\,\middle|\,\begin{matrix}\boldsymbol{q}\\ j\end{matrix}\right)e^*_\beta\left(k\,\middle|\,\begin{matrix}\boldsymbol{q}\\ j\end{matrix}\right)+m_{k'}^{-1}e_\alpha\left(k'\,\begin{matrix}\boldsymbol{q}\\ j\end{matrix}\right)e^*_\beta\left(k'\,\middle|\,\begin{matrix}\boldsymbol{q}\\ j\end{matrix}\right)\right]-\right.$$

$$\left.-\varphi^{kk'}_{\alpha\beta\gamma\varepsilon\delta\varrho}(\boldsymbol{q})\,(m_k m_{k'})^{-1/2}\left[e_\alpha\left(k\,\middle|\,\begin{matrix}\boldsymbol{q}\\ j\end{matrix}\right)e^*_\beta\left(k'\,\middle|\,\begin{matrix}\boldsymbol{q}\\ j\end{matrix}\right)+e_\alpha\left(k'\,\middle|\,\begin{matrix}\boldsymbol{q}\\ j\end{matrix}\right)e^*_\beta\left(k\,\middle|\,\begin{matrix}\boldsymbol{q}\\ j\end{matrix}\right)\right]\right\} \tag{7}$$

and the Fourier transform of the fourth derivative

$$\varphi^{kk'}_{\alpha\beta\gamma\varepsilon\delta\varrho}(\boldsymbol{q})=\sum_{l-l'}\varphi_{\alpha\beta\gamma\delta}\begin{pmatrix}l\,l'\\ kk'\end{pmatrix}x_\varepsilon\begin{pmatrix}l\,l'\\ kk'\end{pmatrix}x_\varrho\begin{pmatrix}l\,l'\\ kk'\end{pmatrix}\mathrm{e}^{i\boldsymbol{q}\boldsymbol{x}\binom{ll'}{kk'}}; \tag{8}$$

additional contributions of third order are

$$C^{(3)}_{\alpha\beta\gamma\delta}(T)=2\hbar\,\frac{1}{Nv_\mathrm{a}}\sum_{\boldsymbol{q}j\neq j'}\gamma^{jj'}_{\alpha\beta}(\boldsymbol{q})\,\gamma^{jj'}_{\delta\gamma}(\boldsymbol{q})\,\frac{\omega^2\left(\begin{matrix}\boldsymbol{q}\\ j\end{matrix}\right)\omega\left(\begin{matrix}\boldsymbol{q}\\ j'\end{matrix}\right)\left[2n\left(\begin{matrix}\boldsymbol{q}\\ j'\end{matrix}\right)+1\right]}{\omega^2\left(\begin{matrix}\boldsymbol{q}\\ j'\end{matrix}\right)-\omega^2\left(\begin{matrix}\boldsymbol{q}\\ j\end{matrix}\right)}, \tag{9}$$

$$C^{(4)}_{\alpha\beta\gamma\delta}(T)=-\frac{\hbar}{2}\,\frac{1}{Nv_\mathrm{a}}\sum_{\boldsymbol{q}j}\gamma^{jj}_{\alpha\beta}(\boldsymbol{q})\,\gamma^{jj}_{\gamma\delta}(\boldsymbol{q})\,\omega\left(\begin{matrix}\boldsymbol{q}\\ j\end{matrix}\right)\left[2n\left(\begin{matrix}\boldsymbol{q}\\ j\end{matrix}\right)+1\right], \tag{10}$$

$$C^{(5)}_{\alpha\beta\gamma\delta}(T)=-\frac{\hbar^2}{k_\mathrm{B}T}\,\frac{1}{Nv_\mathrm{a}}\sum_{\boldsymbol{q}j}\gamma^{jj}_{\alpha\beta}(\boldsymbol{q})\,\gamma^{jj}_{\gamma\delta}(\boldsymbol{q})\,\omega^2\left(\begin{matrix}\boldsymbol{q}\\ j\end{matrix}\right)n\left(\begin{matrix}\boldsymbol{q}\\ j\end{matrix}\right)\left[n\left(\begin{matrix}\boldsymbol{q}\\ j\end{matrix}\right)+1\right]. \tag{11}$$

With the aid of isothermal elastic constants the first and zero sound values are developed by adding additional frequency dependent terms.

In the first sound case with adiabatic propagation we have to take account of the difference between isothermal and adiabatic elastic constants that was developed e.g. by Cowley [1] and by Niklasson [3].

$$C^{(6)}_{\alpha\alpha\alpha\alpha}(T)=C^{(6)}_{\alpha\alpha\beta\beta}(T)=\frac{\hbar^2}{k_\mathrm{B}T}\,\frac{1}{Nv_\mathrm{a}}\,\frac{\left[\sum_{\boldsymbol{q}j}\gamma\left(\begin{matrix}\boldsymbol{q}\\ j\end{matrix}\right)n\left(\begin{matrix}\boldsymbol{q}\\ j\end{matrix}\right)\left[n\left(\begin{matrix}\boldsymbol{q}\\ j\end{matrix}\right)+1\right]\omega^2\left(\begin{matrix}\boldsymbol{q}\\ j\end{matrix}\right)\right]^2}{\sum_{\boldsymbol{q}j}n\left(\begin{matrix}\boldsymbol{q}\\ j\end{matrix}\right)\left[n\left(\begin{matrix}\boldsymbol{q}\\ j\end{matrix}\right)+1\right]\omega^2\left(\begin{matrix}\boldsymbol{q}\\ j\end{matrix}\right)}, \tag{12}$$

$$C^{(6)}_{\alpha\beta\alpha\beta}(T)=0\,. \tag{13}$$

Finally the first sound elastic constants are defined by

$$C^{\text{1. sound}}_{\alpha\beta\gamma\delta}(T)=C^{\mathrm{is}}_{\alpha\beta\gamma\delta}(T)+C^{(6)}_{\alpha\beta\gamma\delta}(T)\,. \tag{14}$$

When calculating zero sound elastic constants the finite lifetimes of the thermal phonons may be neglected. As a consequence the contribution $C^{(5)}_{\alpha\beta\gamma\delta}(T)$ is the only one to exhibit significant changes. Thus it is substituted when zero sound elastic constants are to be evaluated [1]

$$C^{\text{0. Sound}}_{\alpha\beta\gamma\delta}(T,\,\Omega\boldsymbol{Q})=C^{\mathrm{is}}_{\alpha\beta\gamma\delta}(T)-C^{(5)}_{\alpha\beta\gamma\delta}(T)+C^{(7)}_{\alpha\beta\gamma\delta}(T,\,\Omega\boldsymbol{Q}) \tag{15}$$

with

$$C^{(7)}_{\alpha\beta\gamma\delta}(T, \Omega\boldsymbol{Q}) = \frac{\hbar^2}{k_B T}\frac{1}{2Nv_a}\sum_{\boldsymbol{q}j}\gamma^{jj}_{\alpha\beta}(\boldsymbol{q})\,\gamma^{jj}_{\gamma\delta}(\boldsymbol{q})\,n\left(\frac{\boldsymbol{q}}{j}\right)\left[n\left(\frac{\boldsymbol{q}}{j}\right)+1\right]\omega^2\left(\frac{\boldsymbol{q}}{j}\right)\times$$

$$\times\left\{\frac{\boldsymbol{Q}\cdot\nabla_{\boldsymbol{q}}\omega\left(\frac{\boldsymbol{q}}{j}\right)}{\left[\Omega-\boldsymbol{Q}\cdot\nabla_{\boldsymbol{q}}\omega\left(\frac{\boldsymbol{q}}{j}\right)\right]_P}-\frac{\boldsymbol{Q}\cdot\nabla_{\boldsymbol{q}}\omega\left(\frac{\boldsymbol{q}}{j}\right)}{\left[\Omega+\boldsymbol{Q}\cdot\nabla_{\boldsymbol{q}}\omega\left(\frac{\boldsymbol{q}}{j}\right)\right]_P}\right\}. \tag{16}$$

Actually we see that the zero sound elastic constants are depending on the probe frequency Ω and on the direction of propagation of the sound wave $\boldsymbol{Q}$.

So far we have treated the pure first and zero sound regimes. However, in order to compare elastic constants being determined from different experimental techniques with theoretical investigations, it is necessary to have more detailed knowledge about the transition region. Lack of information about this intermediate region often makes it impossible to decide whether the condition for zero sound holds for all frequencies in an inelastic neutron scattering experiment or whether Brillouin data refer to the first sound region.

Following Niklasson [3] we obtain

$$C_{\alpha\beta\gamma\delta}(T, \Omega\boldsymbol{Q}) = C^{\mathrm{is}}_{\alpha\beta\gamma\delta}(T) + \frac{\hbar^2}{k_B T}\frac{1}{2Nv_a}\sum_{\boldsymbol{q}j}\gamma^{jj}_{\alpha\beta}(\boldsymbol{q})\,\gamma^{jj}_{\gamma\delta}(\boldsymbol{q})\,n\left(\frac{\boldsymbol{q}}{j}\right)\left[n\left(\frac{\boldsymbol{q}}{j}\right)+1\right]\omega^2\left(\frac{\boldsymbol{q}}{j}\right)\times$$

$$\times\left\{\frac{\Omega}{\Omega-\boldsymbol{Q}\cdot\nabla_{\boldsymbol{q}}\omega\left(\frac{\boldsymbol{q}}{j}\right)+2i\Gamma}+\frac{\Omega}{\Omega+\boldsymbol{Q}\cdot\nabla_{\boldsymbol{q}}\omega\left(\frac{\boldsymbol{q}}{j}\right)+2i\Gamma}\right\}. \tag{17}$$

In the low-frequency limit we receive from the above expression the isothermal elastic constants. This is exact for transverse branches and neglects the difference between isothermal and adiabatic elastic constants for longitudinal branches. In the high-frequency limit $\Omega \gg \Gamma$ we receive the zero sound result.

3. Numerical Results

The calculations are based on a breathing shell model for the phonon dispersion that was determined from inelastic neutron scattering by Raunio and Rolandson [11] for RbI and by Buyers [9] for NaF. The modifications proposed by Kress [13] for the ratio of the breathing and shell–core spring have been included. The third potential derivatives have been determined from an analysis of the experimental averaged Grüneisen constants and thermal expansion data for both crystals. For RbI experimental results by Schuele and Smith [17] and White [18] and for NaF results by James and Yates [19] and by Pathak et al. [20] were used. The theory of microscopic Grüneisen parameters has been worked out in recent papers by Jex [12] and Kress [13] on the basis of the breathing shell model. In case of RbI also the dispersion of microscopic Grüneisen parameters is available from the neutron scattering data by Blaschko et al. [14]. In the further numerical work of this paper we use the theory of Jex to describe the Grüneisen tensor $\gamma^{jj'}_{\alpha\beta}(\boldsymbol{q})$ without Coulomb anharmonicity in order to save computer time. It has been shown [12] that this neglection only changes the $\gamma\left(\frac{\boldsymbol{q}}{j}\right)$ of the TA-branch in the [100] direction significantly. In summary only one free parameter φ^{III} is

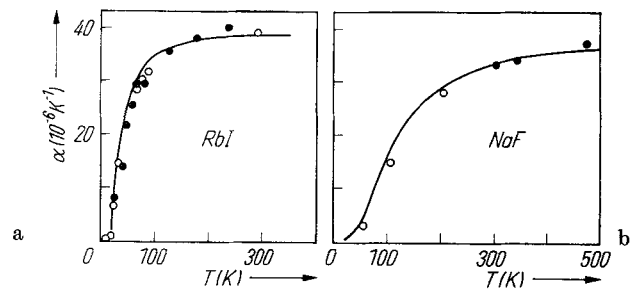

Fig. 1. Calculated coefficient of linear thermal expansion compared with experiments. a) Experiments in RbI by Schuele and Smith [17] (●) and by White [18] (○). b) Experiments in NaF by James and Yates [19] (○) and by Pathak et al. [20] (●)

left to adjust the coefficient of linear thermal expansion over the whole temperature range. The results of such calculations are presented in Fig. 1a and 1b. In Fig. 2 we have drawn the related microscopic Grüneisen parameters of NaF; the agreement with the optical data by Mitra et al. [21] is consistent. Corresponding curves of RbI are discussed in [12, 13, 14]. The parameter φ^{IV} which is needed for the mass operator calculation was determined from assuming a Born-Mayer ansatz $\varphi = Ae^{-ar}$ between nearest neighbours. The constants A, a were determined from the ratio $(\varphi^{II}/\varphi^{III})$. φ^{II} was taken from the lattice dynamics calculation. The potential parameters are summarized in Table 1.

After this determination of realistic input parameters, we concentrate on the temperature dependence of the first and zero sound elastic constants. The first sound elastic constants can be compared directly with temperature dependent ultrasound experiments in these crystals. We therefore evaluated equation (14). Summations in the Brillouin zone have been extended over 4000 q-points. It is important to notice that the different contributions (equation (2), (6), (9), (10), (11), (12)) due to thermal expansion, three- and four-phonon processes and difference between adiabatic and isothermal elastic constants contribute with dif-

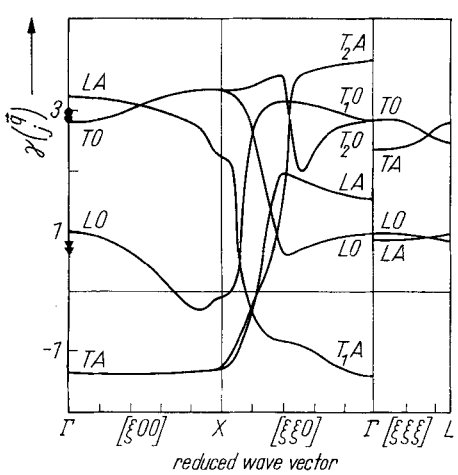

Fig. 2. Dispersion of the mode Grüneisen parameters in NaF at $T = 295$ K. Longitudinal (▼) and transverse (●) optical data by Mitra et al. [21]

Table 1
Derivatives of the nearest-neighbour interaction potential in RbI and NaF

derivative	RbI	NaF	units
$\frac{1}{r}\varphi^{I}$	−0.925	−0.774	$e^2/2v$
φ^{II}	13.86	10.57	$e^2/2v$
φ^{III}	−143.2	−93.17	$e^2/2vr$
φ^{IV}	1494	821.1	$e^2/2vr^2$

ferent signs. The results of the temperature dependent first sound elastic constants are presented in Fig. 3. Especially for RbI the agreement between theory and ultrasonic experiments is excellent for C_{11} and satisfactory for C_{12} and C_{44}. The harmonic elastic constants $C^{\text{harm}}_{\alpha\beta\gamma\delta}(0)$ of equation (1) were chosen such that the adiabatic constants fit the experiments at 80 K. Actually different signs of the temperature gradients are accurately reproduced by the theory.

The temperature dependence of the zero sound elastic constants results from (15). In this case the elastic constants depend on the applied frequency and the wave vector $\boldsymbol{Q}$. This fact has also been pointed out by Cowley [1]. The gradients $\nabla_{\boldsymbol{q}}\omega\begin{pmatrix}\boldsymbol{q}\\ j\end{pmatrix}$ which determine the contribution equation (16) were evaluated from the well-known method of Gilat and Dolling [22]. The real part equation (16) and the imaginary part being the Hilbert transform of this equation, are plotted in Fig. 4 for the $\boldsymbol{Q} = (0.2, 0, 0)$ phonon. The shape of the mass operator is similar to Cowley's calculation in KBr [1]. The afore-mentioned violation of the second rank tensor symmetry [1] of the zero sound elastic constants turns out to be rather small (less than 1%) and may be neglected. In Fig. 5 the temperature dependent contributions of the first and zero sound elastic constants are represented for both crystals under investigation. The zero

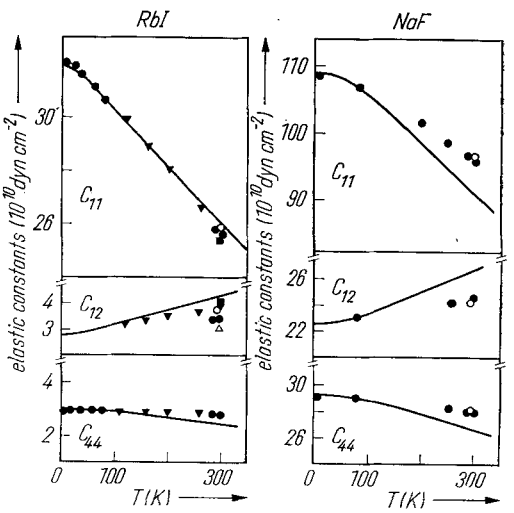

Fig. 3. Calculated temperature dependent first sound eleastic constants compared with ultrasonic measurements. (△ Bolof and Menes [23], ○ Haussühl [24], ■ Reinitz [25], ● Lewis et al. [26], ▼ Ghafelehbashi et al. [27])

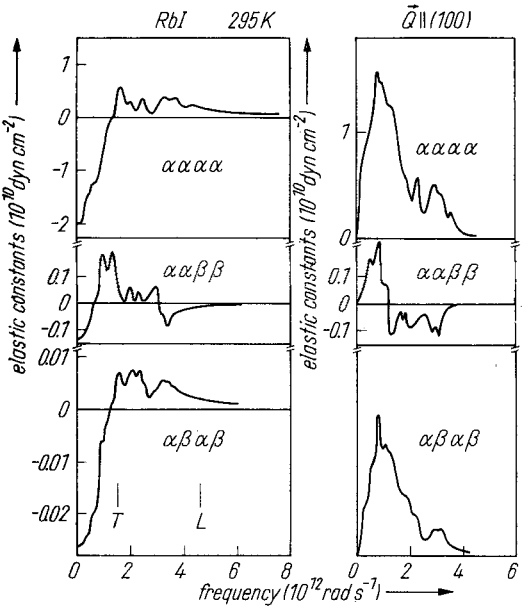

Fig. 4. Real and imaginary part of the frequency dependent anharmonic contribution to the elastic constants in the zero sound region of RbI, $T = 295$ K, $\boldsymbol{Q} \parallel (100)$

sound elastic constants were evaluated from the [ξ00] LA, [ξ00] TA and [ξξ0] T_2A branches at $q/q_{max} = 0.2$.

In Table 2 we compare first sound elastic constants given by an average over the ultrasonic data (RbI: Bolef and Menes [23], Haussühl [24], Reinitz [25], Lewis et al. [26], Ghafelehbashi et al. [27], Chang and Barsch [28]; NaF: Haussühl [24], Lewis et al. [26]) with isothermal and zero sound elastic constants calculated according to equations (14) and (15). Table 3 shows the theoretical differences between zero and first sound elastic constants at room temperature compared with experimental results where we subtracted the ultrasonic values from recent neutron scattering data by Loidl et al. [10], Loidl [29] and Buyers [9]. The elastic constants from the neutron scattering experiments [10, 29] were deduced from the slopes of the dispersion curves in a wave vector region $0.1 \leqq q/q_{max} \leqq 0.2$ and corrected for nonlinear effects of the dispersion with the breathing shell model. So far we have discussed the two extreme situations of pure first sound and pure zero sound; however, it seems also important to treat the intermediate region $\Omega \approx \Gamma$. This has been done in a microscopic picture in papers by Sham [30], Klein and Wehner [31] and Niklasson [3] and others. From these investigations an interpolation formula in terms of Green's functions has been worked out (equation (17)) that covers both regions in the limit

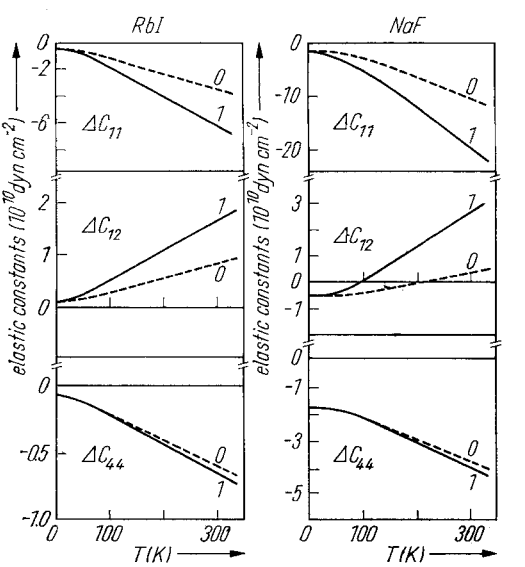

Fig. 5. Comparison of the temperature dependent contributions to the first sound (full line) and to the zero sound (broken line) elastic constants

Table 2

First sound elastic constants from an average over the ultrasonic data [23 to 28] compared with theoretical isothermal and zero sound elastic constants*)

RbI	C_{11}	C_{12}	C_{44}
first sound	25.66	3.64	2.793
isothermal sound	25.10	3.08	2.793
zero sound	28.23	3.01	2.827
NaF	C_{11}	C_{12}	C_{44}
first sound	96.8	24.5	28.08
isothermal sound	94.54	22.24	28.08
zero sound	105.26	22.36	28.28

*) All values are at room temperature; the units are 10^{10} dyn cm^{-2}.

Table 3

Theoretical differences between zero and first sound elastic constants compared with experimental results*)

RbI	ΔC_{11}	ΔC_{44}	$\Delta\left(\frac{C_{11}-C_{12}}{2}\right)$	ΔC_{12}
theory	2.43	0.04	1.60	−0.63
exp. [29]	2.3	0.06	1.3	−0.4
NaF	ΔC_{11}	ΔC_{44}	$\Delta\left(\frac{C_{11}-C_{12}}{2}\right)$	ΔC_{12}
theory	8.5	0.2	5.3	−2.1
exp. [9]	12.1	1.7	6.3	−0.5
exp. [10]		−0.1	4.9	

*) The average of the ultrasonic data is subtracted from neutron scattering data. The units are 10^{10} dyn cm^{-2}.

$\Omega \gtrless \Gamma$ and also approximates the complicated ladder diagrams [1, 3]. This equation (17) describes transverse acoustic branches completely over the frequency range Ω, while for longitudinal branches the adiabatic-isothermal correction must be added. This correction however is only important in the collision dominated region and is negligible for frequencies $\Omega \gg \Gamma$. The predictions of the theory can be checked directly with the neutron experiments by Loidl et al. [10] covering the intermediate region at different temperatures in NaF. From an analysis of these data it can be concluded that the concept of an averaged

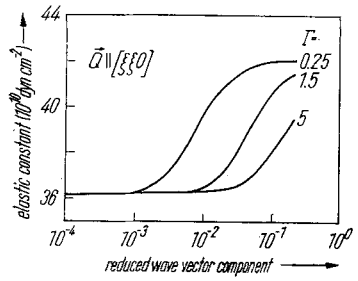

Fig. 6. Transition region of the elastic constant $C'' = \frac{1}{2}(C_{11} - C_{12})$ in NaF for various widths of the averaged inverse lifetime (in 2π THz) of the thermal phonons, $T = 295$ K

wave vector independent width Γ of the thermal phonons of the crystal works quite well. Such an averaged width Γ is also involved in the thermal conductivity data. Fig. 6 demonstrates the influence of different Γ-values on the elastic constant $C'' = \frac{1}{2}(C_{11} - C_{12})$ as a function of the wave vector $\boldsymbol{Q}$ in the transition region of NaF. In Fig. 7 the same symmetry direction is presented for RbI. The averaged Γ was deduced from thermal conductivity data [32] to $\Gamma/2\pi = 0.018$ THz at room temperature. The calculations show that the transition region is located typically around $Q = (0.01$ to $0.1)\, 2\pi/a$ in the Brillouin zone. This region can be covered with inelastic neutron scattering. In Fig. 8 we have fitted the experiments in NaF at four temperatures 295, 500, 600, 700 K of the sound velocities [10, 29] with (17). The averaged Γ-values and the deduced isothermal elastic constants are listed in Table 4. A more sophisticated analysis gave slightly modified results compared with our previous publication [10]. Fig. 8 also shows the shift of the transition region towards larger q-values with rising temperature. The experimental results are excellently interpreted by the theory.

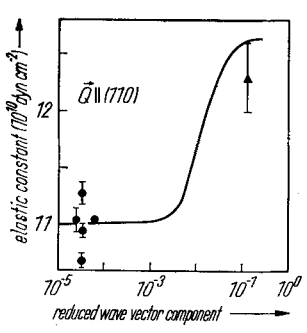

Fig. 7

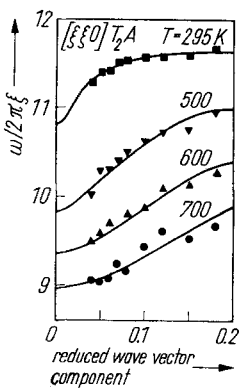

Fig. 8

Fig. 7. Wave vector dependence of the elastic constants $C'' = \frac{1}{2}(C_{11} - C_{12})$ in RbI ($T = 295$ K). The averaged $\Gamma/2\pi = 0.018$ THz was deduced from thermal conductivity data. The theoretical results (—) are compared with ultrasonic data ● [24 to 28] and with inelastic neutron scattering ▲ [29]; $\boldsymbol{Q} \parallel (\xi\, \xi\, 0)$

Fig. 8. Sound velocities (in units of THz × lattice constant/$\sqrt{2}$) in NaF in the transition region between zero and first sound. Neutron data by Loidl et al. [10]

Table 4

Averaged inverse phonon lifetimes and isothermal elastic constants deduced from inelastic neutron data in the transition region

temperature (K)	$\left(\frac{C_{11}-C_{12}}{2}\right)$ (10^{10} dyn cm^{-2})	$\Gamma/2\pi$ (THz)
295	35.3	0.16
500	28.9	0.48
600	26.1	0.80
700	23.8	1.11

4. Discussion

The transition region between first and zero sound in NaF and RbI has been investigated in detail starting from the pure limits of collision dominated and collisionless regimes in the crystals. This investigation was stimulated by recent neutron experiments covering the transition region at different temperatures up to 700 K in NaF [10]. The theoretical knowledge about the lattice dynamics and lattice anharmonicity is rather elevated due to the phonon dispersion analysis [9, 11, 13] and determination of the anharmonic coupling parameters in terms of Grüneisen constants [12, 13, 14]. It has been shown from the analysis in NaF that the averaged width Γ independent of the phonon wave number $\boldsymbol{q}$ is sufficient to explain the magnitude and the position of the transition region. We believe that the determination of the phonon width is rather sensitive and perhaps more accurate than from thermal conductivity experiments. Γ-values of NaF are listed in Table 4 for different temperatures. NaF is important to investigate because it is the first alkali halide where second sound has successfully been observed. One aspect of the experiments that has been pointed out in a recent analysis of the phonon lifetime of the probe should be persued further [33]. Theory predicts the width to be temperature independent in the first sound regime. This enables experimentalists to observe phonon resonances at high temperatures where normal phonons in the zero sound regime are damped out to a large extent. The interpretation of the first sound widths might give information about the viscosity tensor and the thermal conductivity tensor in these crystals [34]. The decrease of phonon lifetimes with rising temperatures has been demonstrated in NaF in the transition region near the first sound and was discussed in a paper by Loidl et al. [33].

From the analysis of zero sound phonon measurements by Loidl [29] in symmetry and off-symmetry of RbI (more than 300 phonons) we conclude that the deviation between zero and first sound elastic constants was overestimated in Raunio's earlier experiments [11] which were not specialized to that region of the Brillouin zone. Our results which are consistent with the calculations are listed in Table 2.

Acknowledgement

This research was supported by the Bundesministerium für Forschung und Technologie.

References

[1] R. A. Cowley, Proc. Phys. Soc. **90**, 1127 (1967).
[2] M. Blinick and H. J. Maris, Phys. Rev. B **2**, 2139 (1970).
[3] G. Niklasson, Phys. kondens. Materie **14**, 138 (1972).
[4] R. Nava, R. Callarotti, H. Ceva, and A. Martinet, Phys. Rev. **185**, 1177 (1969).
[5] J. Hasson and A. Many, Phys. Rev. Letters **35**, 792 (1975).
[6] E. C. Svensson and W. J. L. Buyers, Phys. Rev. **165**, 1063 (1968).
[7] H. E. Jackson, D. Landheer, and B. P. Stoicheff, Phys. Rev. Letters **31**, 296 (1973).
D. Landheer, H. E. Jackson, R. A. McLaren, and B. P. Stoicheff, Phys. Rev. B **13**, 888 (1976).
[8] G. Dolling, H. G. Smith, R. M. Nicklow, P. R. Vijayaraghavan, and M. K. Wilkinson, Phys. Rev. **168**, 970 (1968).
[9] W. J. L. Buyers, Phys. Rev. **153**, 923 (1967).
[10] A. Loidl, J. Daubert, and E. Schedler, J. Phys. C **9**, L33 (1976).
[11] G. Raunio and S. Rolandson, phys. stat. sol. **40**, 749 (1970).
[12] H. Jex, phys. stat. sol. (b) **62**, 393 (1974).
[13] W. Kress, phys. stat. sol. (b) **62**, 403 (1974).
W. Kress and H. Jex, phys. stat. sol. (b) **71**, 577 (1975).
[14] O. Blaschko, G. Ernst, G. Quittner, W. Kress, and R. E. Lechner, Phys. Rev. B **11**, 3960 (1975).
[15] H. Beck, Z. Phys. B **21**, 209 (1975).
[16] E. R. Cowley and R. A. Cowley, Proc. Roy. Soc. **A287**, 259 (1965).
[17] D. E. Schuele and C. S. Smith, J. Phys. Chem. Solids **25**, 801 (1964).
[18] G. K. White, Proc. Roy. Soc. **A286**, 204 (1965).
[19] B. W. James and B. Yates, Phil. Mag. **12**, 253 (1965).
[20] P. D. Pathak, N. V. Pandya, and M. P. Ghadiali, Indian J. Phys. **27**, 293 (1963).
[21] S. S. Mitra, C. Postmus, and J. R. Ferraro, Phys. Rev. Letters **18**, 455 (1967).
[22] G. Gilat and G. Dolling, Phys. Letters **8**, 304 (1964).
[23] D. I. Bolef and M. Menes, J. appl. Phys. **31**, 1010 (1960).
[24] S. Haussühl, Z. Phys. **159**, 223 (1960).
[25] K. Reinitz, Phys. Rev. **123**, 1615 (1961).
[26] T. Lewis, A. Lehoczky, and C. V. Briscoe, Phys. Rev. **161**, 877 (1967).
[27] M. Ghafelehbashi, D. P. Dandekar, and A. C. Ruoff, J. appl. Phys. **41**, 652 (1970).
[28] Z. P. Chang and G. R. Barsch, J. Phys. Chem. Solids **32**, 27 (1971).
[29] A. Loidl, Thesis, Universität Frankfurt/Main 1976.
[30] L. J. Sham, Phys. Rev. **156**, 494 (1967).
[31] P. Klein and R. K. Wehner, Phys. kondens. Materie **8**, 141 (1968); **10**, 1 (1969).
[32] J. P. Moore, R. K. Williams, and R. S. Graves, Phys. Rev. B **11**, 3107 (1975).
[33] A. Loidl, J. Daubert, H. Jex, and E. Schedler, Phys. Letters. A **56**, 139 (1976).
[34] R. Paetsch, phys. stat. sol. (b) **71**, 557 (1975).